

Interpretable travel distance on the county-wise COVID-19 by sequence to sequence with attention

Ting Tian^{a,1}, Yukang Jiang^{a,1}, Huajun Xie^{a,1}, Xueqin Wang^{b,c,2}, and Hailiang Guo^{d,2}

^aSchool of Mathematics, Sun Yat-sen University

^bSchool of Management, University of Science and Technology of China

^cSchool of Statistics, Capital University of Economics and Business, 121 Zhangjialukou, Huaxiang Fengtai District, Beijing 100070, China

^dNingxia University, Yinchuan 750021, Ningxia, China

Abstract

Background: Travel restrictions as a means of intervention in the COVID-19 epidemic have reduced the spread of outbreaks using epidemiological models. We introduce the attention module in the sequencing model to assess the effects of the different classes of travel distances.

Objective: To establish a direct relationship between the number of travelers for various travel distances and the COVID-19 trajectories. To improve the prediction performance of sequencing model.

Setting: Counties from all over the United States.

¹Ting Tian, Yukang Jiang, and Huajun Xie contributed equally to this article

²Corresponding authors: Xueqin Wang; Hailiang Guo

Participants: New confirmed cases and deaths have been reported in 3158 counties across the United States.

Measurements: Outcomes included new confirmed cases and deaths in the 30 days preceding November 13, 2021. The daily number of trips taken by the population for various classes of travel distances and the geographical information of infected counties are assessed.

Results: There is a spatial pattern of various classes of travel distances across the country. The varying geographical effects of the number of people travelling for different distances on the epidemic spread are demonstrated.

Limitation: We examined data up to November 13, 2021, and the weights of each class of travel distances may change accordingly as the data evolves.

Conclusion: Given the weights of people taking trips for various classes of travel distances, the epidemics could be mitigated by reducing the corresponding class of travellers.

Primary Funding Source: National Natural Science Foundation of China.

1. INTRODUCTION

Since March 2020, the novel coronavirus disease (COVID-19) has been declared a pandemic by the World Health Organization ([WHO Director General, 2020](#)) and is rapidly spreading throughout the world. As of November 13, 2021, the United States was responsible for one-fifth of all confirmed global cases and one-seventh of total global deaths, with over 47 million cumulative confirmed cases and 0.76 million total deaths. Throughout the early 2020 pandemic, every public health authority had activated an escalating response. On March 19, 2020, California, for example, implemented the “stay home except for essential needs” order. However, the number of travellers had gradually increased prior to the appearance of SARS-CoV-2.

According to the Bureau of Transportation Statistics (<https://www.bts.gov/daily-travel>), there are ten different travel distances that represent how far people travel when they leave home. They track trips ranging from less than a mile to more than 500 miles. Over 16 billion and approximately 12 billion people travelled in 2019 and 2020. Nonetheless, until December 2021, the number of trips was approximately 15.2 billion. To simplify the presentation, we first classify travellers by their original ten types of travel distances into four categories based on three geographical scales (i.e., 1 mile, 50 miles, and 250 miles). There are four types of trips: less than 1 mile, between 1 and 50 miles, between 50 and 250 miles, and more than 250 miles. They are referred to as “community-,” “county-,” “in-state-,” and “out-of-state-” travel distances. Thus, we observe their nationwide daily change in the United States from 2019 to 2021.

From 2019 to 2021, Figure 1 depicts the daily change pattern of people who are taking trips over a wide range of travel distances in the United States. The change in travel distance is defined as the relative difference in the daily number of people taking trips for each class of travel distance from January to December in 2019 over 2020, 2020 over 2021, and 2019 over 2021 when compared to the same period from January to December in the previous year. Since March 2020, the number of people taking trips across the entire range of travel

distances has begun to decline, but the number of people taking trips across “county-level” travel distances (between 50 and 250 miles) has gradually increased since May 2020, when compared to the same periods in 2019. The number of people making trips for “community-level” travel distances (i.e., trips less than 1 mile) has decreased for nearly a year (from March 2020 to February 2021), and the number of people making trips has resumed to its pre-pandemic level after February 2021. During the year 2021, it appears that people have gradually returned to their regular daily routines. There is a strikingly distinct nationwide change pattern for people who travel long distances that can be observed across a wide range of distances.

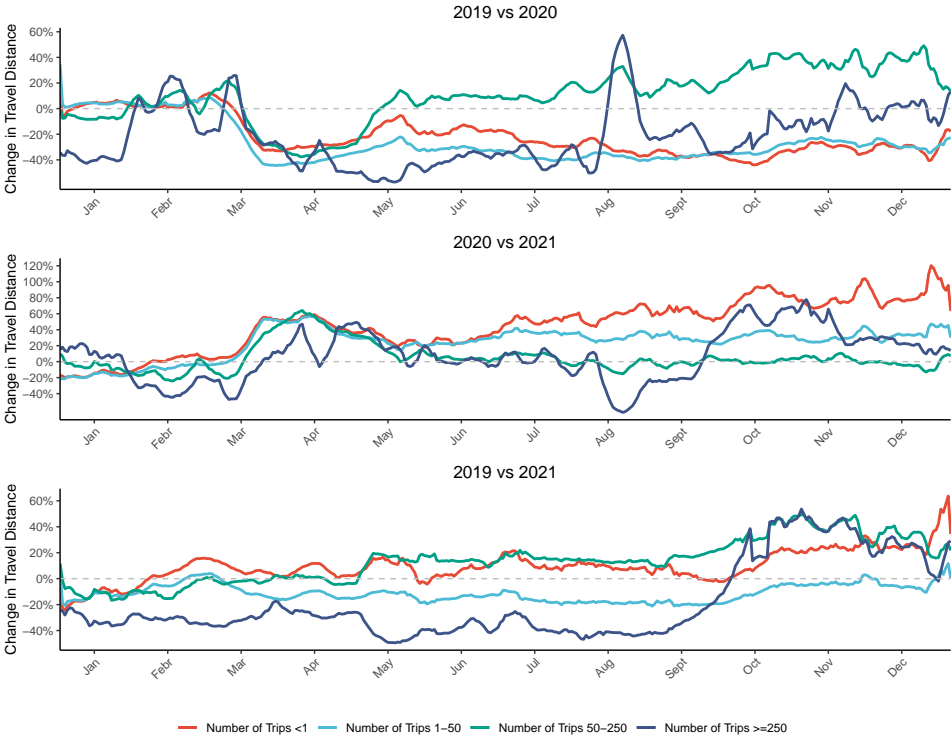


Figure 1: Relative nationwide travel distance changes (daily change from 2019 to 2021) in the United States.

Travel distance is a measure of mobility, and travel bans serve to slow transmission. Numerous researchers have emphasized the importance of reducing mobility in order to prevent transmission by reducing the effective reproduction number (Flaxman et al., 2020;

Dehning et al., 2020; Jia et al., 2020). Chinazzi et al. (2020) simulated various levels of travel restriction, thereby mitigating the Chinese epidemic. Additionally, some authors developed a mobility network to simulate the effects of movement restrictions in France, Italy, and the United Kingdom (Galeazzi et al., 2021) and of the lockdown-induced changes in Germany (Schlosser et al., 2020). Both epidemiological models and mobility networks concur on the benefits of reduced mobility. However, it remains unclear which class of travel distance poses the greatest constraint on the epidemic spread and whether the spatio-temporal distribution of travel distance affects both confirmed cases and deaths. The daily number of trips taken by the population, which records various travel distances across all counties in the United States, enables the modelling of the various travel distances on epidemic trajectories.

Deep learning, as an emerging science, is being used to great effect in all spheres of life (Ronneberger et al., 2015; Ren et al., 2015; Hochreiter and Schmidhuber, 1997; Sutskever et al., 2014). Many sequence-based deep learning methods have demonstrated high prediction accuracy for COVID-19 (Pang et al., 2021; Zhang-James et al., 2021; Tian et al., 2021). Alassafi et al. (2022) compare and evaluate the performance of various prediction models for COVID-19 cases, recovered COVID-19 cases, and deaths. It makes a seven-day forecast with a high degree of accuracy. However, most of these methods rely on sequential models in deep learning to forecast future unintelligible epidemic trajectories (Chandra et al., 2022; Sinha et al., 2022). Furthermore, the approaches do not consider geographic information in favour of directly predicting epidemic trajectories using time series data. Nevertheless, geographic information significantly affects the prediction and analysis results (Giuliani et al., 2020; Tian et al., 2021). The existing deep learning articles analyse and forecast primarily at the state (Chandra et al., 2022) or even at the national level (Sinha et al., 2022), with little or no modelling at the smaller county level. Thus, we incorporate county-level patterns of travel distances into a sequence-based deep learning framework to demonstrate the qualitative effects of the number of trips taken by the population on epidemic spread in general.

To measure the weights of different travel distances, we propose an epidemic-free model

and investigate the effect of the pattern of change in travel distance on the spatio-temporal spread of COVID19. The sequence-to-sequence learning framework (Sutskever et al., 2014) and attention-based learning (Fukui et al., 2019) are used in conjunction to provide a data-driven approach that improves sequence forecasting accuracy and improves the interpretability of travel distances. These are the inputs to the model, which include the sequence of epidemic trajectories with past confirmed cases and deaths and the number of people who travel for various travel distances. In addition, for COVID-19, we incorporate geographical information (latitude and longitude) (Tian et al., 2021) and state information to predict the sequence of events in the future. Most importantly, we want to determine the relationship between travel patterns and the number of new cases and deaths. The specific class of travel distance is more important in determining epidemic spread than the overall distance travelled. As a result, the unique goal of our research is to provide an intuitive travel pattern for predicting and interpreting the course of an epidemic at various times and locations throughout the United States, which could aid decision-makers in improving the COVID-19’s mobility rule.

2. MATERIALS AND METHODS

2.1 Data sources

We track the daily number of new confirmed cases and deaths in each infected county in the United States from the first-day patients were confirmed to November 13, 2021. The New York Times provided the epidemic data (The New York Times, 2021). In addition, the daily number of trips made by the population across four categories of travel distances is collected concurrently with epidemic data (<https://www.bts.gov/daily-travel>). There are 3118 counties in 50 states where epidemic and travel data are available. The geographic coordinates of each infected county (longitude and latitude) are derived from Census TIGER 2000 (National Oceanic And Atmospheric Administration, 2022).

2.2 Data usage

To evaluate the performance of our proposed model, we randomly divide 3118 counties into training and test counties, with a 4:1 ratio of training to test counties. Additionally, we validate our model from the date confirmed cases were first reported officially in a county in the United States to November 2021. As a result, the last seven and thirty days of COVID-19's trajectory prior to November 13, 2021, are predicted. Figure 2 illustrates the county-level data structure used for time projection and region validation. The total length of a red and green bar represents the period from the first day cases were reported in a United States county to November 13, 2021. For every 30 days, the blue bars depict observed epidemic data (including cases and deaths) and four classes of travel distances during the same period as the input data. The yellow bars represent the projected cases and deaths in a county for the following 7- (or 30- day) period. In order for the last yellow bar to appear, COVID-19 must have completed its last 7- or 30-day trajectory before November 13, 2021. Each county begins at a different time than the others, but they all end at the same time. This results in variations in the total length of input data across the counties studied.

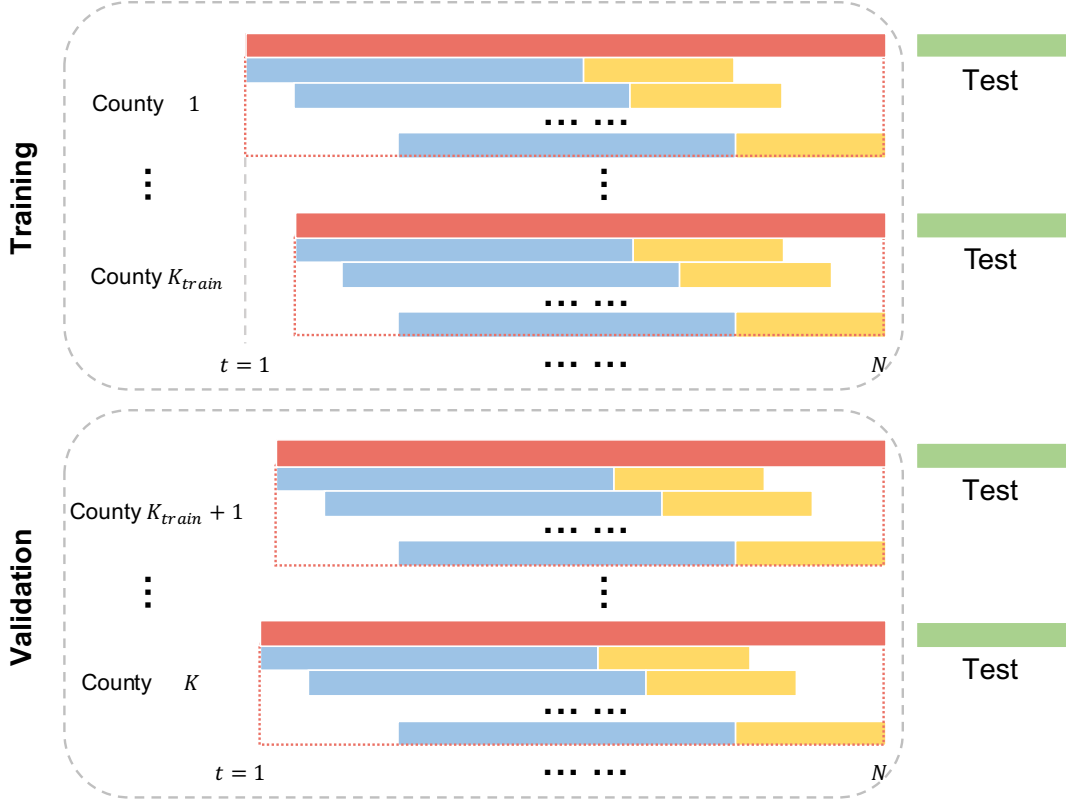


Figure 2: The structure of data usage in the proposed model.

The expression for the inputs of the epidemic data (E) are:

$$\mathbf{X}_{..k}^{(E)} = \begin{pmatrix} x_{1,k}^{(cases)} & \cdots & x_{30,k}^{(cases)} & x_{1,k}^{(deaths)} & \cdots & x_{30,k}^{(deaths)} \\ \vdots & \cdots & \cdots & \cdots & \cdots & \vdots \\ x_{N-37,k}^{(cases)} & \cdots & x_{N-8,k}^{(cases)} & x_{N-37,k}^{(deaths)} & \cdots & x_{N-8,k}^{(deaths)} \end{pmatrix}_{T \times 60}, k = 1, 2, \dots, K$$

where N is the length of the training period, $T = N - 30$, and K is the total number of counties. $x_{i,k}^{(cases)}$ are the new confirmed cases and $x_{i,k}^{(deaths)}$ are the new deaths at the corresponding date. For example, $i = 1$ corresponds to the first day when the confirmed cases were officially reported in a county. These new confirmed cases and deaths give rise to 60 historical epidemic variables as the first part of the input data.

Also, we define the travel distance data (D) as:

$$\mathbf{D}_{..k} = \begin{pmatrix} d_{1,1,k} & d_{1,2,k} & d_{1,3,k} & d_{1,4,k} \\ \vdots & \vdots & \vdots & \vdots \\ d_{N,1,k} & d_{N,2,k} & d_{N,3,k} & d_{N,4,k} \end{pmatrix}_{N \times 4}, k = 1, 2, \dots, K.$$

The columns of $\mathbf{D}_{..k}$ are the number of the population taking “community-level” (less than 1 mile), “county-level” (between 1 mile and 50 miles), “in-state-level” (between 50 miles and 250 miles), and “out-state-level” (over 250 miles) trips, respectively. These 4 variables of travel distances as the second part of the input data.

Taking 7-day for example, the corresponding predicted cases and deaths are:

$$\mathbf{Y}_k = \begin{pmatrix} x_{31,k}^{(cases)} & \dots & x_{37,k}^{(cases)} & x_{31,k}^{(deaths)} & \dots & x_{37,k}^{(deaths)} \\ \vdots & \dots & \dots & \dots & \dots & \vdots \\ x_{N-7,k}^{(cases)} & \dots & x_{N,k}^{(cases)} & x_{N-7,k}^{(deaths)} & \dots & x_{N,k}^{(deaths)} \end{pmatrix}_{T \times 14}, k = 1, 2, \dots, K$$

2.3 Attention-Net

We predict the subsequent 7- and 30-day new trajectories of COVID-19 by combining past epidemic data incorporating new cases and deaths with the same period of travel distance data. Our fundamental model is a sequence-to-sequence framework based on an encoder-decoder structure, with Long Short-Term Memory (LSTM) as the building block ([Hochreiter and Schmidhuber, 1997](#)). We begin by introducing LSTM. The structure of LSTM is composed of a cell state c_t , an input gate in_t , a forget gate f_t , and an output gate o_t . Given a sequence of multivariate variables $\{x_1, x_2, \dots, x_t\}$, where $x_t \in \mathbb{R}^d$, we calculate the hidden

state h_t as follows:

$$\begin{aligned}
i_t &= \sigma(W_i x_t + U_i h_{t-1} + b_i) \\
f_t &= \sigma(W_f x_t + U_f h_{t-1} + b_f) \\
o_t &= \sigma(W_o x_t + U_o h_{t-1} + b_o) \\
\tilde{c}_t &= \tanh(W_c x_t + U_c h_{t-1} + b_c) \\
c_t &= f_t \odot c_{t-1} + i_t \odot \tilde{c}_t \\
h_t &= o_t \odot \tanh(c_t),
\end{aligned}$$

where σ and \odot denote the sigmoid function and element-wise multiplication, respectively. Here, x_t is defined as $\text{Concat}(\mathbf{X}_{t,k}^{(E)}, \text{Attention}(D_{t,k}))$, and let Concat be the process of concatenate in the deep learning and Attention be the attention module, which are discussed below.

In the following step, we create a framework for sequence-to-sequence conversion, which falls under the broad category of the encoder-decoder structure. According to (Sutskever et al., 2014), it is capable of converting one sequence into another sequence, albeit where the lengths of the input and output sequences can differ. There have been studies that have used a sequence-to-sequence architecture to predict COVID-19 in the past (Pang et al., 2021; Zhang-James et al., 2021). Their work, however, was primarily focused on predicting epidemic trends rather than providing information for decision-makers. The designed attention module is therefore included in our basic model, allowing us to calculate the quantitative impact of travel distances on the spread.

The attention module is used to learn the weights of each variable and each time step $\alpha_t \in \mathbb{R}^{30 \times 4}$. The travel distance data and the geographical information including the latitude and longitude, and the state information (state ID) are fused in the attention module. Specifically, the categorical variable of state ID is transformed by an embedding layer for feature representations, whereas the continuous variables of latitudes and longitudes are transformed by a linear layer. An h -dimension vector represents each geographical variable.

They are combined by means of a concatenation operation to yield the global geographical information representation, g_k , $k = 1, \dots, K$, and there are different representations for different counties.

Each travel distance data sample $\mathbf{d}_t \in \mathbb{R}^{30 \times 4}$ contains 30 rows representing the every 30-day period, and 4 columns representing the number of trips taken by the population over four different distance classes. It is flattened and transformed by a linear layer in the same way as the representations

$$\mathbf{d}_t^{(r)} = \begin{pmatrix} d_{t,1}^{(r)\top} \\ \vdots \\ d_{t,30}^{(r)\top} \end{pmatrix}_{30 \times (4h)} .$$

We combine the geographical information by

$$\eta_{t,j} = \text{BN}(W_d \cdot d_{t,j}^{(r)} + b_d) + \text{BN}(W_g \cdot (g_k) + b_g), \quad j = 1, \dots, 30, \quad t = 1, \dots, N - 30,$$

where $W_d, W_g \in \mathbb{R}^{4 \times 4h}$ are the weights, and $b_d, b_g \in \mathbb{R}^{4 \times 1}$ are constants. BN is a batch normalization layer.

Consequently, the weights of the population taking trips for each class of travel distance are normalized and added together to give a total weight of one. We use “elu” and “tanh” to enhance the model’s expression capability following the linear layer and the “softmax” activation function to control the output ranges between 0 and 1. The attention weights can be calculated using the following formula:

$$\alpha_{t,j} = \text{softmax}(f(\eta_{t,j})), \quad j = 1, 2, \dots, 30,$$

where f is composed of a linear layer and tanh is an activation function. We have the following formula to aggregate the travel distance data and calculate the context vector

$$v = [v_1, v_2, \dots, v_{30}],$$

$$v_{t,j} = \sum_i^4 \alpha_{t,j,i} d_{t,j,i}.$$

After $v_{t,j}$ are obtained, we concatenate them with $\mathbf{X}_{..k}^{(E)}$ as the transformed data into the encoder and predict \mathbf{Y}_k in the decoder. Thus, each 30-day epidemic and travel distance data set becomes the encoder’s transformed inputs, and the decoder generates 7- and 30-day predicted epidemic trajectories as outputs. Figure 3 depicts the proposed structure of the deep neural network in its entirety. The proposed model is referred to as an attention-net.

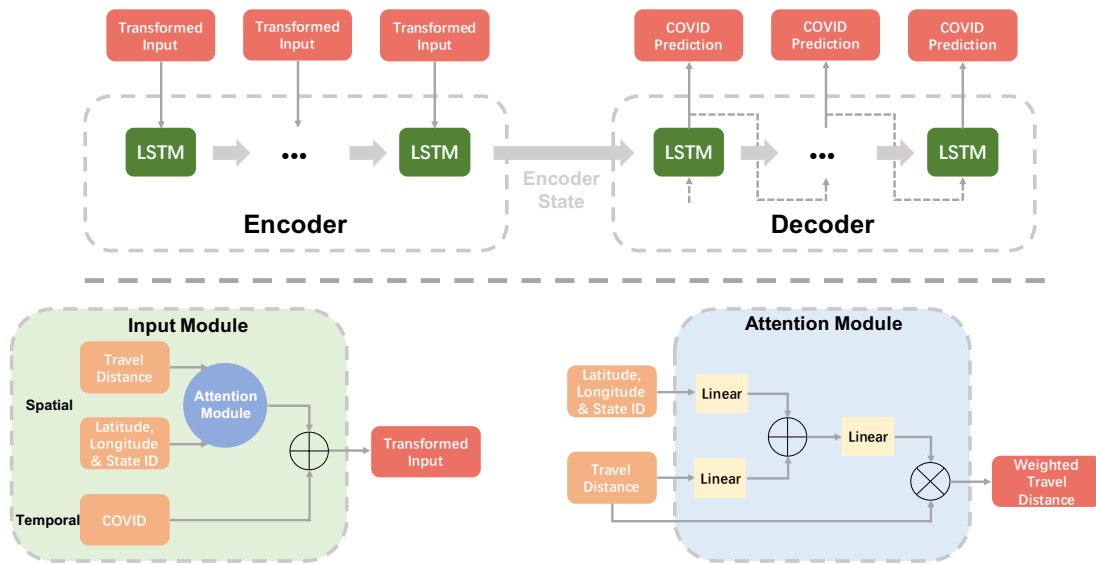


Figure 3: The structure of an attention-net. The upper panel is the primary model with an encoding and decoding structure, and the lower panels are the input and attention modules, respectively.

2.4 Implementation details

We implement an attention-net with the Keras 2.6. The detailed network configurations and training procedure for each module in the attention-net are as follows:

- There are 256 nodes and dropout regularization with a probability of 0.2 in the LSTM layer. The details of nodes and the dropout regularization are described in [Tian et al. \(2021\)](#).

- The dimension h of the hidden vector in the attention module equals to 64.
- For training practice, we use the stochastic gradient descent (SGD) with an initial learning rate of 0.1 and a stepped decay rate of 0.1 every 40 epochs for a total of 200 epochs. To avoid overfitting, we employ an early stopping strategy.
- The loss function is a root-mean-square error (RMSE) to measure the accuracy of the attention-net: $RMSE = \sqrt{\frac{\sum_{i=1}^t (Predicted_i - Observed_i)^2}{t}}$, $t = 7, 30$, where $Predicted_i$ are the predicted new confirmed cases or new deaths at the i^{th} day, and $Observed_i$ are the observed ones at the same corresponding date.

3. RESULTS

3.1 Prediction performance

We use the test data (represented by the green bars in Figure 2) to validate the prediction performance of attention-net and calculate RMSE to compare our model with sequence-to-sequence model alone.

- Sequence-to-sequence: encoder input data is $\text{Concat}(\mathbf{X}_{t,k}^{(E)}, D_{t,k})$.
- Attention-net: encoder input data is $\text{Concat}(\mathbf{X}_{t,k}^{(E)}, \text{Attention}(D_{t,k}))$.

We present a summary of the average values of RMSEs for 3118 infected counties. The $RMSE_7$ and $RMSE_{30}$ of new cases and new deaths for the attention-net are 354.029, 852.085 and 0.412, 0.529, respectively. The corresponding $RMSE_7$ and $RMSE_{30}$ for sequence-to-sequence only model are 433.423, 1281.237, and 0.416, 0.631, respectively. The values of RMSEs for our proposed model are lower than those for sequence-to-sequence model alone, indicating that our attention-net model outperforms in terms of prediction. To further demonstrate the accuracy of the county-level prediction for attention-net, we plot the last 7- and 30- day predicted and observed new cases and new deaths before November 13, 2021,

for four representative counties (See Appendix Figure 1). These four representative counties are chosen based on their relatively higher average weights over the entire period for the population taking trips for each of four classes of travel distances (See Table 1). Their population densities are also on the higher end of the scale.

3.2 Spatial effects of travel distances on COVID-19

Table 1: The different 10 counties with the relatively higher average weights over the entire period for the population taking trips for each of four classes of travel distances.

“Community-level” Trips (< 1 mile)		“County-level” Trips (between 1 and 50 miles)		“In-state-level” Trips (between 50 and 250 miles)		“Out-state-level” Trips (> 250 miles)	
Counties	Weights	Counties	Weights	Counties	Weights	Counties	Weights
California Riverside	0.7002	Hawaii Honolulu	0.3489	Illinois Cook	0.5354	Florida Glades	0.3740
California San Bernardino	0.6943	Alaska Nome Census Area	0.3351	Alaska Fairbanks North Star Borough	0.5148	Florida Monroe	0.3734
California Los Angeles	0.6658	Alaska Kodiak Island Borough	0.3286	Alaska Southeast Fairbanks Census Area	0.5146	Florida Hendry	0.3713
Texas Harris	0.6198	Washington Wahkiakum	0.3243	Alaska Yukon-Koyukuk Census Area	0.5146	Florida Okeechobee	0.3701
California San Diego	0.5970	Alaska Bethel Census Area	0.3242	Alaska Matanuska-Susitna Borough	0.5145	Florida Hardee	0.3700
California San Joaquin	0.5944	Alaska Fairbanks North Star Borough	0.3211	Alaska Anchorage	0.5084	Florida DeSoto	0.3698
Texas Bexar	0.5937	Washington Jefferson	0.3205	Alaska Juneau City and Borough	0.5058	Florida Martin	0.3627
California Orange	0.5807	Washington Skamania	0.3203	Alaska Nome Census Area	0.4989	Florida Highlands	0.3627
California Kern	0.5792	Alaska Yukon-Koyukuk Census Area	0.3203	Alaska Kenai Peninsula Borough	0.4986	Florida Indian River	0.3611
Texas Tarrant	0.5536	Washington Pacific	0.3196	Alaska Petersburg Borough	0.4967	Florida Charlotte	0.3608

Table 1 examines how average weights in the number of trips taken by the population for four different types of travel distances vary by geography. For example, compared to other states, 7 counties in California have fairly higher average weights for “community-level” trips (extremely short travel distances), while 10 counties in Florida have relatively higher average weights for “out-state-level” trips (long travel distances). Additionally, 9 counties in Alaska have slightly higher average weights for “in-state-level” trips (intermediate travel distances). Overall, the top 10 average weights for the population taking “community-level” trips are considerably greater than the average weights for the population taking the remaining travel distance classes

Referring back to Figure 2 of the Appendix, it should be noted that four representative counties are chosen, and we look at their average weights over 30 days before November 13, 2021, for a full range of the population taking trips in each of those counties. The

estimated average weights of the population taking “community-level”, “county-level”, “in-state-level” and “out-state-level” trips are 0.6451, 0.1112, 0.1325, and 0.1112 for California, Los Angeles County, 0.3690, 0.3610, 0.1123, and 0.1577 for Hawaii Honolulu County, 0.1219, 0.1184, 0.6626, and 0.097 for Illinois, Cook County, and 0.3427, 0.1814, 0.1190, and 0.3569 for Florida, Indian River County, respectively. Particularly notable is that the average weights for the two classes of travel distances in Honolulu (“community-level” and “county-level”) and Indian River (“community-level” and “out-state-level”) Counties are almost exactly equal. In comparison, Los Angeles (“community-level”) and Cook (“in-state-level”) Counties have disproportionately larger average weights for a class of distance travelled. This hints at the spatial distribution of travel distances in infected counties.

For the overall spatial distribution of travel distances in the 3118 infected counties of the United States (Figure 4), the estimated average weights over the entire period could conceivably vary by geography. For example, with the exception of Ocean County in New Jersey and Suffolk County in New York, the infected counties in the northern region have relatively larger average weights for the population taking “in-state-level” trips than the rest of the region. These two counties, as well as the majority of counties in the south-western region, have relatively higher average weights of the population taking “community-level” trips. The average weights for each class of travel distance over the entire period for each infected county have class-specific changes and are spatially different for each class of travel distance.

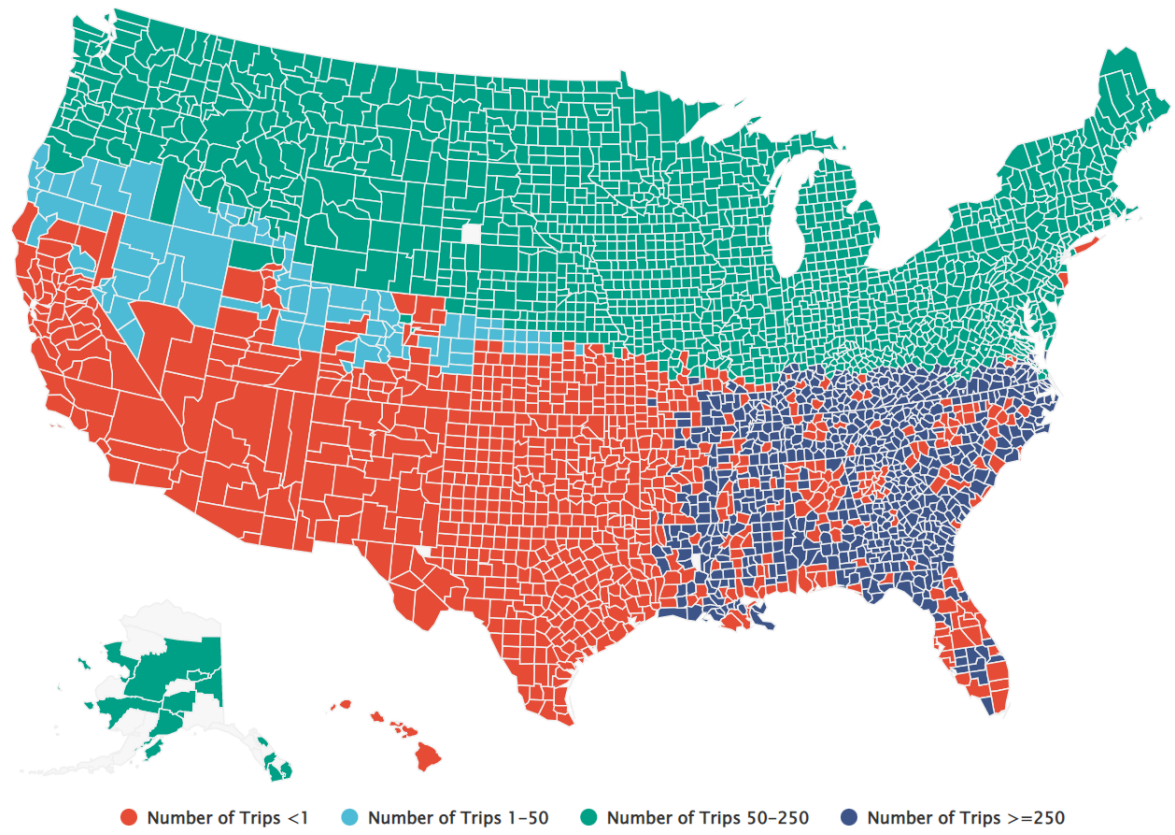


Figure 4: The map of the spatial distribution of average weights over the entire period for a full range of travel distances in 3118 infected counties of the United States.

3.3 Temporal effects of travel distances on COVID-19

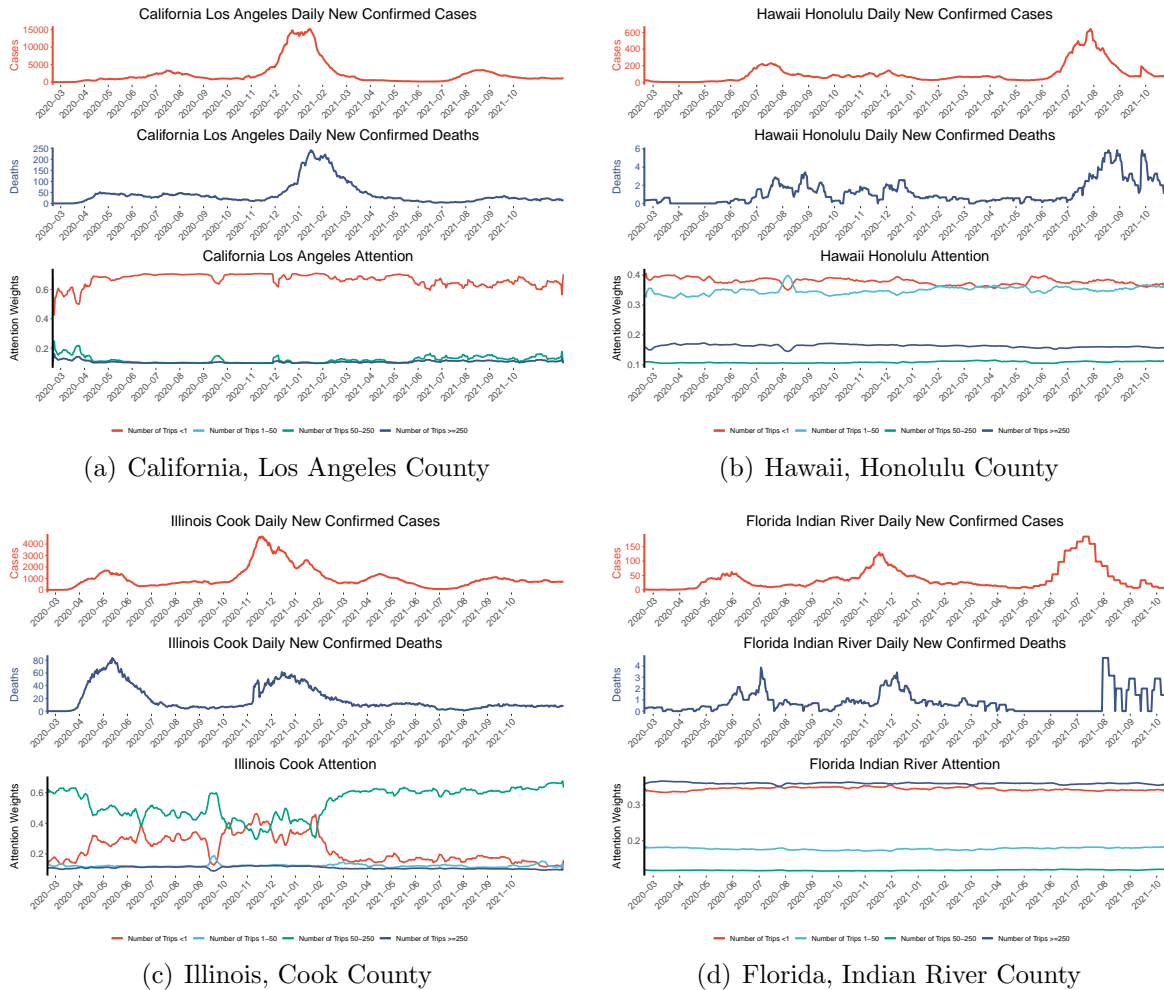


Figure 5: The trajectories of COVID-19 (new cases and new deaths) and the trend of estimated weights for a full range of travel distances across the entire period in California Los Angeles, Hawaii Honolulu, Illinois Cook, and Florida Indian River.

Apart from spatial distinctions, we are interested in the temporal distribution of travel distances. COVID-19 trajectories (new cases and deaths) and estimated daily weights for a representative sample of the population travelling from the first day confirmed cases were reported to October 2021 in California Los Angeles, Hawaii Honolulu, Illinois Cook, and Florida Indian River are depicted in Figure 5. The estimated weights for each class of travel distance in Honolulu and Indian River counties have remained relatively stable on a daily basis. Every day, the weights for the population taking “community-level” trips always

outweigh those for the population taking trips over longer distances. The daily weights for this population fluctuate at different times of the epidemic and after June 2021 in Los Angeles County. Cook County’s daily weight trajectories, in particular, are qualitatively dynamic for the population making “community-level” and “in-state” trips. Former values were greater than 0.6 at the start of the epidemic, decreased to approximately 0.4 in April 2020, and returned to greater than 0.6 in March 2021. In comparison, the later ones began at 0.2 and gradually increased to 0.4, peaked around November 2020, and finally decreased to less than 0.2 by March 2021.

4. DISCUSSION

Our Attention-network generates two critical characteristics. To begin, county-level sequential 7- and 30-day new cases and deaths are forecast accurately. Second, we estimate the time-varying weights of the population taking “community-level,” “county-level,” “in-state,” and “out-of-state” trips. To be more specific, we develop a deep learning model by including the attention module, which allows us to accurately predict the number of new confirmed cases and deaths in the infected counties of the United States of America. We take advantage of the number of people who travel for four classes of travel distances in order to generate new evidence that can be used to influence the spread of the epidemic and, as a result, inform decision-makers.

Our analysis looks at a variety of different types of travel distances from the start of COVID-19 to November 2021. The number of people travelling decreased early in the pandemic, but the number of people travelling short and intermediate distances began to increase after late May 2020 (Figure 1). This could indicate that the COVID-19 interventions at the beginning of the pandemic were successful in reducing the number of trips made by the population. The policy of resumption of business, on the other hand, was gradually implemented throughout the country. For instance, on May 7, 2020, the state of California issued a directive “reopening lower-risk workplaces and other spaces” ([Office Of Public Affairs, 2020](#)). As

a result, people may be able to recover the distances they travel on a regular basis (known as “community-level” travel distances). This is consistent with Figure 5, which indicates an increase in the number of people making “community-level” trips. Thus, in Los Angeles County, California, their time-varying attention weights are dominated (greater than 0.6 after May 2020). Alternatively, a report stated that Illinois may benefit from tourists seeking shorter distances to travel during the summer of 2020 (Moore, 2020). According to a survey commissioned by the United States Travel Association, approximately one-third of people would travel up to 300 miles for their vacation destination, i.e., regional travel. It is expected that people will change their travel habits voluntarily in response to the COVID-19. Figure 5 depicts an example of this type of travel behavioural change, in which people taking “in-state” trips increased, and their attention weights were found to be relatively higher overall in Cook County, Illinois.

On the basis of the distribution of county-level COVID-19, we discovered a heterogeneous spatial pattern of travel distances. These distinctions can be interpreted in a number of different ways. One possible explanation is that more and more people are choosing to travel by car. As a result, the number of long-distance travellers (such as those who travel by plane) has decreased (Schlosser et al., 2020). The weights of people who travel “out-state-level” are comparatively lower than those of their short-distance counterparts overall. However, when compared to the remaining three classes of travel distances in southern regions, such as Florida state, those weights are relatively higher. Tourism is a year-round socioeconomic activity in Florida, with more than half of all domestic tourists arriving in the state during the year (Kirilenko et al., 2020). As a result, the weights of people travelling for various classes of travel vary geographically. This may vary according to the travel destination’s characteristics. In terms of the temporal pattern of travel distances, we discovered that the weights of all classes do not change significantly over time. However, when COVID19 spread was severe again in Cook County, Illinois, the attention weights assigned to “community-level” trips surpassed those assigned to “in-state-level” trips in late 2020. In general, weight

curves are flattened in regions where the epidemic spread is not severe.

Given the weights of people travelling for various distance classes, epidemics can be mitigated by reducing the corresponding class of travellers. In epidemics, there is a direct relationship between the number of travellers and the spread of the disease. With a thorough understanding of the effects of travel pattern changes, policymakers could effectively control the ongoing COVID-19 spread. Additionally, the framework of our model can be extended to a wide variety of fields, providing not only exceptional precision but also excellent spatio-temporal interpretability.

APPENDIX

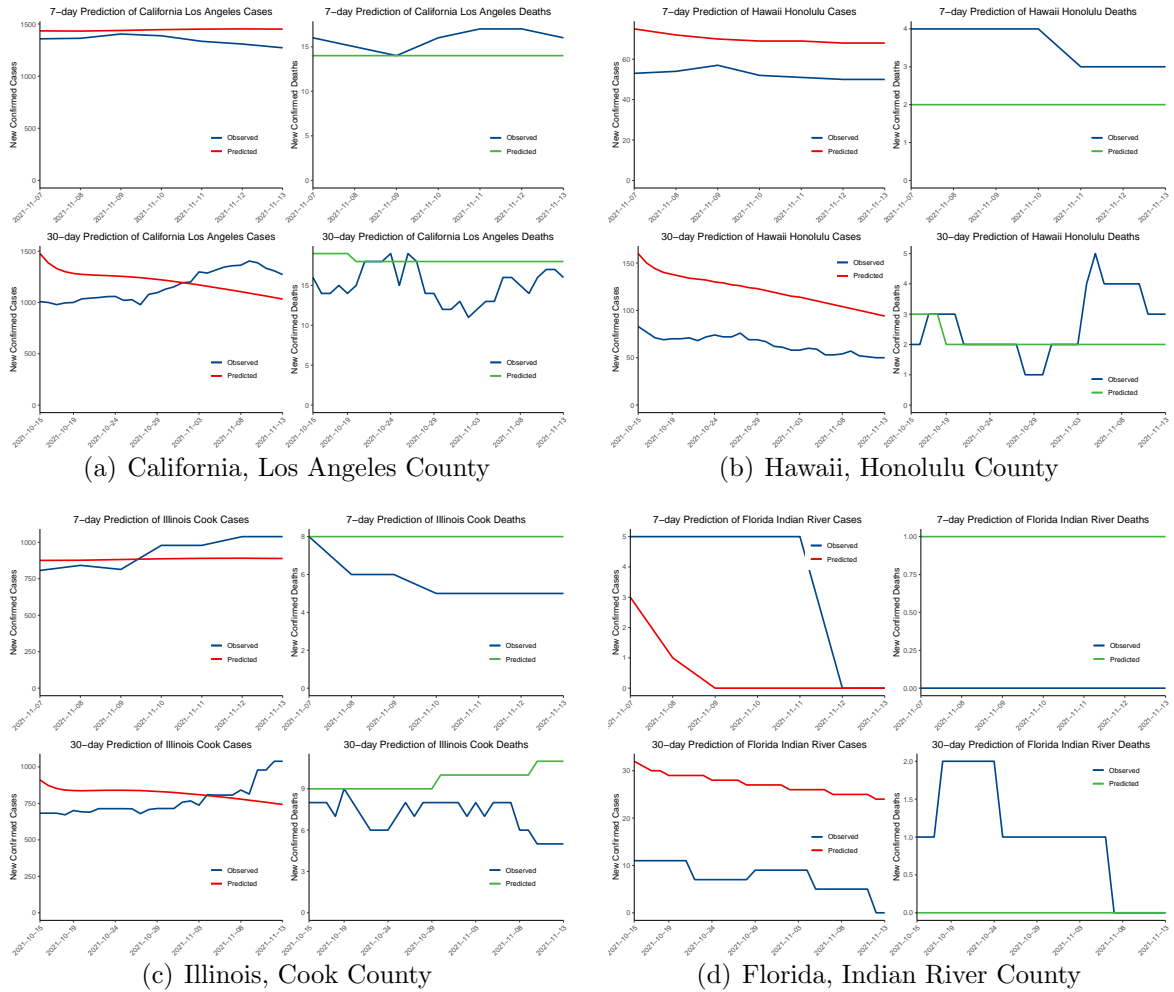


Figure 1: 7- and 30- day new confirmed cases and new deaths prediction of California Los Angeles, Hawaii Honolulu, Illinois Cook, and Florida Indian River.

Figure 1 shows the last 7- and 30- day predicted and observed trajectories of COVID-19 before November 13, 2021. The gaps between predicted and observed new cases and new deaths are very small, respectively, for California Los Angeles, Hawaii Honolulu, Illinois Cook, and Florida Indian River.

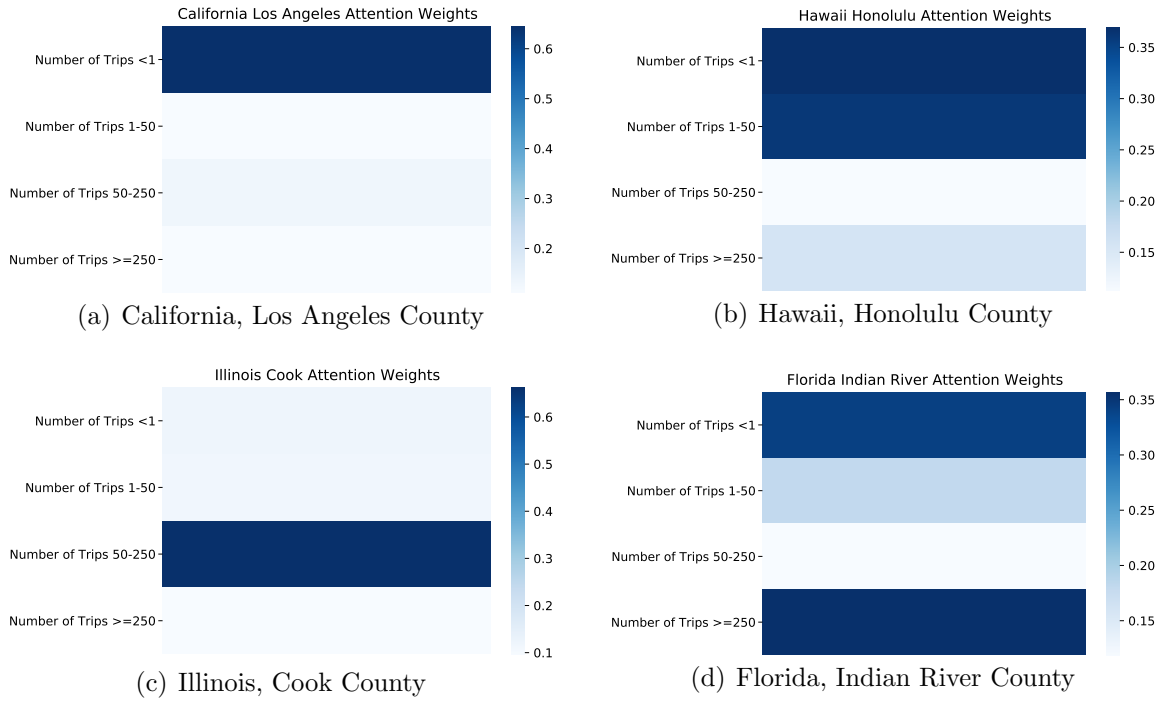


Figure 2: The heatmap of the average weights over the last 30-day before November 13, 2021 for a full range of travel distances in California Los Angeles, Hawaii Honolulu, Illinois Cook, and Florida Indian River.

REFERENCES

- Alassafi, M. O., Jarrah, M., and Alotaibi, R. (2022), “Time series predicting of COVID-19 based on deep learning,” *Neurocomputing*, 468, 335–344.
- Chandra, R., Jain, A., and Singh Chauhan, D. (2022), “Deep learning via LSTM models for COVID-19 infection forecasting in India,” *PloS one*, 17(1), e0262708.
- Chinazzi, M., Davis, J. T., Ajelli, M., Gioannini, C., Litvinova, M., Merler, S., y Piontti, A. P., Mu, K., Rossi, L., Sun, K. et al. (2020), “The effect of travel restrictions on the spread of the 2019 novel coronavirus (COVID-19) outbreak,” *Science*, 368(6489), 395–400.
- Dehning, J., Zierenberg, J., Spitzner, F. P., Wibral, M., Neto, J. P., Wilczek, M., and Priesemann, V. (2020), “Inferring change points in the spread of COVID-19 reveals the effectiveness of interventions,” *Science*, 369(6500).
- Flaxman, S., Mishra, S., Gandy, A., Unwin, H. J. T., Mellan, T. A., Coupland, H., Whitaker, C., Zhu, H., Berah, T., Eaton, J. W. et al. (2020), “Estimating the effects of non-pharmaceutical interventions on COVID-19 in Europe,” *Nature*, 584(7820), 257–261.
- Fukui, H., Hirakawa, T., Yamashita, T., and Fujiyoshi, H. (2019), Attention branch network: Learning of attention mechanism for visual explanation, in *Proceedings of the IEEE/CVF Conference on Computer Vision and Pattern Recognition*, pp. 10705–10714.
- Galeazzi, A., Cinelli, M., Bonaccorsi, G., Pierri, F., Schmidt, A. L., Scala, A., Pammolli, F., and Quattrociochi, W. (2021), “Human mobility in response to COVID-19 in France, Italy and UK,” *Scientific Reports*, 11(1), 1–10.
- Giuliani, D., Dickson, M. M., Espa, G., and Santi, F. (2020), “Modelling and predicting the spatio-temporal spread of COVID-19 in Italy,” *BMC infectious diseases*, 20(1), 1–10.
- Hochreiter, S., and Schmidhuber, J. (1997), “Long short-term memory,” *Neural computation*, 9(8), 1735–1780.

- Jia, J. S., Lu, X., Yuan, Y., Xu, G., Jia, J., and Christakis, N. A. (2020), “Population flow drives spatio-temporal distribution of COVID-19 in China,” *Nature*, 582(7812), 389–394.
- Kirilenko, A., Kim, J. W., Ma, S., Yang, E. et al. (2020), Identification of Tourist Flows in Florida to Support Development of Tourist Travel Module for FDOT Florida Transportation Model,, Technical report, Florida. Department of Transportation.
- Moore, B. (2020), “Illinois could benefit as tourists seek to travel shorter distances,”, <https://www.sj-r.com/story/business/travel/2020/05/30/illinois-could-benefit-as-tourists/1129527007/>.
- National Oceanic And Atmospheric Administration (2022), “U.S. Counties,”, <https://www.weather.gov/gis/Counties>.
- Office Of Public Affairs (2020), “Order of the state public health officer,”, <https://www.cdph.ca.gov/Programs/CID/DCDC/CDPH%20Document%20Library/COVID-19/SH0%20Order%205-7-2020.pdf>.
- Pang, J., Huang, Y., Xie, Z., Li, J., and Cai, Z. (2021), “Collaborative city digital twin for the COVID-19 pandemic: A federated learning solution,” *Tsinghua science and technology*, 26(5), 759–771.
- Ren, S., He, K., Girshick, R., and Sun, J. (2015), “Faster r-cnn: Towards real-time object detection with region proposal networks,” *arXiv preprint arXiv:1506.01497*, .
- Ronneberger, O., Fischer, P., and Brox, T. (2015), U-net: Convolutional networks for biomedical image segmentation,, in *International Conference on Medical image computing and computer-assisted intervention*, Springer, pp. 234–241.
- Schlosser, F., Maier, B. F., Jack, O., Hinrichs, D., Zachariae, A., and Brockmann, D. (2020), “COVID-19 lockdown induces disease-mitigating structural changes in mobility networks,” *Proceedings of the National Academy of Sciences*, 117(52), 32883–32890.

- Sinha, T., Chowdhury, T., Shaw, R. N., and Ghosh, A. (2022), “Analysis and Prediction of COVID-19 Confirmed Cases Using Deep Learning Models: A Comparative Study,” in *Advanced Computing and Intelligent Technologies* Springer, pp. 207–218.
- Sutskever, I., Vinyals, O., and Le, Q. V. (2014), Sequence to sequence learning with neural networks, in *Advances in neural information processing systems*, pp. 3104–3112.
- The New York Times (2021), “Coronavirus in the U.S.: Latest Map and Case Count,” , <https://www.nytimes.com/interactive/2021/us/covid-cases.html>.
- Tian, T., Jiang, Y., Zhang, Y., Li, Z., Wang, X., and Zhang, H. (2021), “COVINet: A deep learning-based and interpretable prediction model for the county-wise trajectories of COVID-19 in the United States,” *medRxiv*, .
URL: <https://www.medrxiv.org/content/early/2020/05/27/2020.05.26.20113787>
- WHO Director General (2020), “WHO Director-General’s opening remarks at the media briefing on COVID-19 -11 March 2020,” , <https://www.who.int/director-general/speeches/detail/who-director-general-s-opening-remarks-at-the-media-briefing-on-covid-19---11-march-2020>.
- Zhang-James, Y., Hess, J., Salekin, A., Wang, D., Chen, S., Winkelstein, P., Morley, C. P., and Faraone, S. V. (2021), “A seq2seq model to forecast the COVID-19 cases, deaths and reproductive R numbers in US counties,” , .